nrsc

Remote Sensing Applications

P. S. Roy
R. S. Dwivedi
D. Vijayan

National Remote Sensing Centre

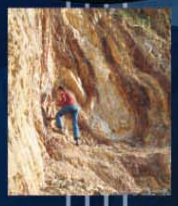

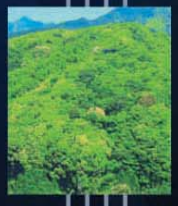

Remote Sensing Applications

Atmosphere

10.1. Introduction

The earth's surface and its near envelope, the atmosphere have provided a unique environment for the evolution and sustenance of plant and animal life on this planet. The present composition of the earth's atmosphere and its surface temperature are the result of an evolutionary process which has involved both the "Geosphere" which includes the land, oceans and the atmosphere and the biologically active region which includes plants and animals, the "Biosphere". The Geosphere Biosphere system is, therefore, a strongly interacting and self regulating system with solar radiation as an external input and a number of internal feed back interactions between its different components make the earth habitable for life. Climate is an important characteristics of the earth system influencing and being influenced by different components the atmosphere, hydrosphere and the biosphere, which determine habitability.

There has been a realization in recent times that the equilibrium of this earth system is being disturbed by a number of natural and anthropogenic factors. Some of them are evolutionary in nature and these are, generally, induced by natural causes e.g., changes in solar radiation flux, changes in earth's orbital parameters etc. But others are of a more short term nature with time scales of decades to centuries and these are largely induced by anthropogenic factors.

The International Geosphere Biosphere Programme (IGBP) launched in 1987 is a programme on global change studies with special reference to climate and environment and is aimed at a detailed study of highly interacting earth system. The scientific objectives of IGBP are: to describe and understand the interactive physical, chemical and biological processes that regulate the total earth system, including the land, oceans and the atmosphere, changes occurring in it and the manner in which they are influenced by human activities.

The main components and drivers of global change are: (i) Changes in land use and land cover; (ii) Global decline in biodiversity; and (iii) Changes in atmospheric composition-CO_2 and other greenhouse gases especially – ozone depletion. The major indicators of global change vis-a-vis human impact are global warming and ozone depletion which have been extensively studied in recent decades.

10.1.1. Greenhouse Effect and Global Warming

The greenhouse effect is a natural phenomenon that occurs when certain gases in the atmosphere, especially water vapor, carbon dioxide and methane, cause the Earth's surface to heat up more than it otherwise would, thereby maintaining a global average temperature warm enough to support life as we know it. Global warming, also called global climate change, occurs when the amounts of carbon dioxide and other trace gases in the atmosphere increase beyond natural levels, thereby intensifying the greenhouse effect. Increased carbon dioxide levels can result from human activities such as the burning of coal, oil and gas and the clearing of forests without replanting.

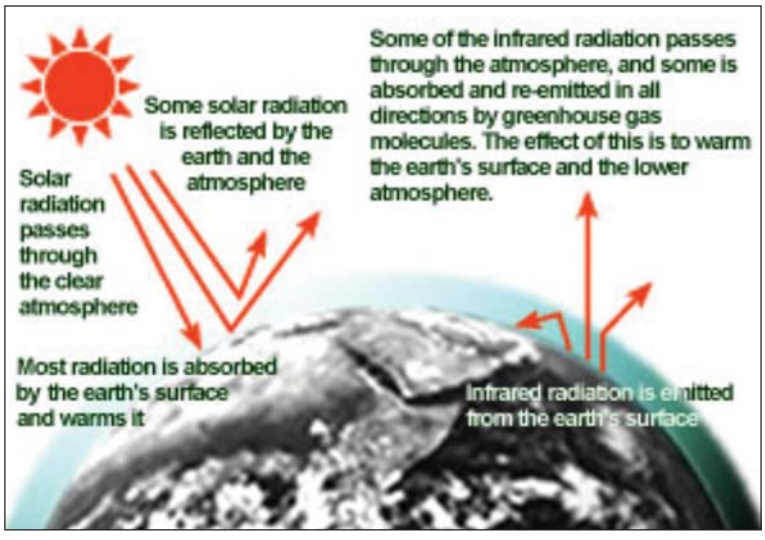

Figure 10.1: Greenhouse effect (source: http://www.gsfc.nasa.gov/gsfc/service/gallery/fact_sheets/earthsci/green.htm; http: //earthobservatory.nasa.gov/Features/Aerosols/)

Greenhouse effect (figure 10.1) is the increase in temperature of the surface of a planet due to the presence of an atmosphere. In the absence of atmosphere, the surface temperature of a planet is determined by the equilibrium between the incident solar radiation flux and the black body emission from the planet surface.

In the presence of an atmosphere, part of the reflected radiation is absorbed by the atmospheric constitutes and re-emitted part of which again reaches the surface thereby increasing the energy available for heating the surface. The result is an increase in the surface temperature and the lower regions of the atmosphere of the planet. The energy balance in the atmosphere is shown here:

The main components in figure 10.2 are the following: Short wavelength (optical wavelengths) radiation from the Sun reaches the top of the atmosphere and clouds reflect ~17% back into space. If the earth gets cloudier, as some climate models predict, more radiation will be reflected back and less will reach the surface. 8% is scattered backwards by air molecules: 6% is actually directly reflected off the surface back into space hence the total reflectivity of the earth is ~31% and this is technically called as albedo. During Ice Ages, Albedo of the earth increased as more of its surface is reflective. The remaining 69% of the incoming radiation that doesn't get reflected back undergoes the following transitions:

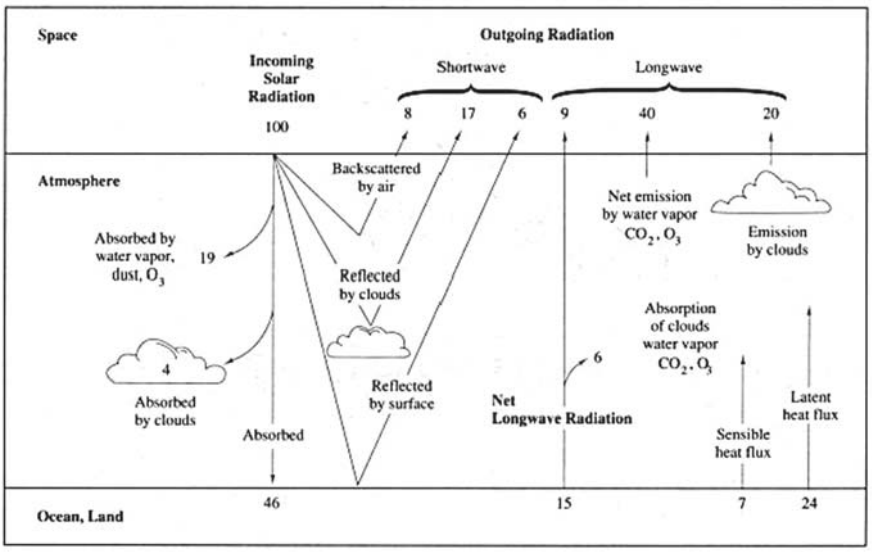

Figure 10.2: The energy balance in the atmosphere(source: http://www.gsfc.nasa.gov/gsfc/service/gallery/fact_sheets/earthsci/green.htm)

- 19% gets absorbed directly by dust, ozone and water vapor in the upper atmosphere. This region is called the stratosphere and is heated by this absorbed radiation. Loss of stratospheric ozone is causing the stratosphere to cool with time, which, of course, greatly confuses the issue of global warming
- 4% gets absorbed by clouds located in the troposphere. This is the lower part of the earth's atmosphere which defines the weather
- The remaining 47% of the sunlight that is incident on top of the earth's atmosphere reaches the surface

This short wavelength radiation absorbed by the earth heats the earth to a finite temperature, it must re-radiate this energy to stay in thermal equilibrium. The earth has an equilibrium temperature of about 300^{o}K. At this temperature, the wavelength of the emitted radiation is mostly in the thermal infrared region. If all the radiation emitted by earth goes directly back into space, the earth would be a significantly colder place than it is. 15% of the long wave radiation is directly radiated back by the cloud-free land surface: 6% of that is absorbed by the atmosphere and 9% goes directly back into space. 60% is re-radiated back into space by the net emission of the atmosphere and the clouds. The total radiated back into space is 69% meaning that 31% is temporarily stored as energy and emitted back later. Of this 31%, 24% is used to facilitate evaporation. This heat is later released through condensation. This process is called latent heat. 7% is stored by the earth's crust and then re-radiated at later through a complicated heat exchange network of convection and conduction. Due to industrial revolution, anthropogenic disturbances caused by human activities increased the ability for the earth's atmosphere to absorb IR radiation causing a net warming of the atmosphere over a period of time. This is the *Enhanced* Greenhouse effect:

Global warming is one of the most serious consequences of development, a major example of environmental degradation over large and temporal scales. It impacts all the components of our environment and the atmosphere, the hydrosphere and the biosphere. The major consequences of global warming are Climate change (Atmosphere); Sea level rise (Hydrosphere) and altered conditions for agriculture (Biosphere).

In addition to these direct effects, there are several indirect effects such as changes in ocean currents and their impact on marine ecosystem, effects on carbon fixing in the oceans and on the land, coral bleaching, changes in ecosystem composition, etc.

10.1.2. Atmospheric Composition

Table 10.1 lists the eleven most abundant gases found in the Earth's lower atmosphere. Of these gases, nitrogen, oxygen, water vapor, carbon dioxide, methane, nitrous oxide and ozone are extremely important to the health of the Earth's biosphere. As evident from the table that nitrogen and oxygen are the main components

of the atmosphere by volume. Together these two gases make up approximately 99% of the dry atmosphere and have very important associations with life. Nitrogen is removed from the atmosphere and deposited at the Earth's surface mainly by nitrogen fixing bacteria, and by way of lightning through precipitation. The addition of this nitrogen to the Earth's surface soils and various water bodies supplies much needed nutrition for plant growth. Nitrogen returns to the atmosphere primarily through biomass combustion and denitrification.

Oxygen is exchanged between the atmosphere and life through the processes of photosynthesis and respiration. Photosynthesis produces oxygen when carbon dioxide and water are chemically converted into glucose in the presence of sunlight. Respiration is the opposite process of photosynthesis. In respiration, oxygen is combined with glucose to chemically release energy for metabolism. The products of this reaction are water and carbon dioxide.

The next most abundant gas is water vapor. Water vapor varies in concentration in the atmosphere both spatially and temporally. The highest concentrations of water vapor are found near the equator over the oceans and tropical rain forests. Cold polar areas and subtropical continental deserts are locations where the volume of water vapor can approach zero percent. Water vapor has several important functional roles on our planet:

- It redistributes heat energy on the Earth through latent heat energy exchange
- The condensation of water vapor creates precipitation that falls on to the Earth's surface providing fresh water for plants and animals
- It helps warm the Earth's atmosphere through the greenhouse effect

The fifth most abundant gas in the atmosphere is carbon dioxide. The volume of this gas has increased by over 35% in the last three hundred years (Table-10.1). This increase is primarily due to human induced burning from fossil fuels, deforestation, and other forms of land-use change. Carbon dioxide is an important greenhouse gas. The human-caused increase in its concentration in the atmosphere has strengthened the greenhouse effect and has definitely contributed to global warming over the last 100 years. Carbon dioxide is also naturally exchanged between the atmosphere and life through the processes of photosynthesis and respiration.

Table 10.1: Average composition of the atmosphere upto an altitude of 25 km.

Gas Name	Chemical Formula	Percent Volume
Nitrogen	N_2	78.08%
Oxygen	O_2	20.95%
*Water	H_2O	0 to 4%
Argon	Ar	0.93%
*Carbon Dioxide	CO_2	0.0360%
Neon	Ne	0.0018%
Helium	He	0.0005%
*Methane	CH_4	0.00017%
Hydrogen	H_2	0.00005%
*Nitrous Oxide	N_2O	0.00003%
*Ozone	O_3	0.000004%

* variable gases

Methane is a very strong greenhouse gas. Since 1750, methane concentrations in the atmosphere have increased by more than 150%. The primary sources for the additional methane added to the atmosphere (in order of importance) are: rice cultivation; domestic grazing animals; termites; landfills; coal mining; and oil and gas extraction. Anaerobic conditions associated with rice paddy flooding results in the formation of methane gas. However, an accurate estimate of how much methane is being produced from rice paddies has been difficult to ascertain. More than 60% of all rice paddies are found in India and China where scientific data concerning emission rates are not available. Nevertheless, scientists believe that the contribution of rice paddies is large because this form of crop production has more than doubled since 1950. Grazing animals release methane to the environment as a result of herbaceous digestion. Some researchers believe the addition of methane from this source has more than quadrupled over the last century. Termites also release methane through similar processes. Land-use change in the tropics, due to deforestation, ranching, and farming, may be causing termite numbers to expand. If this assumption is correct, the contribution from these insects may be important. Methane is also released from landfills, coal mines, and gas and oil drilling. Landfills produce methane as organic wastes decompose over time. Coal, oil, and natural gas deposits release methane to the atmosphere when these deposits are excavated or drilled.

The average concentration of the nitrous oxide is now increasing at a rate of 0.2 to 0.3% per year. Its contribution in the enhancement of the greenhouse effect is minor relative to the other greenhouse gases already mentioned.

However, it does have an important role in the artificial fertilization of ecosystems. In extreme cases, this fertilization can lead to the death of forests, eutrophication of aquatic habitats, and species exclusion. Sources for the increase of nitrous oxide in the atmosphere include: land-use conversion; fossil fuel combustion; biomass burning; and soil fertilization. Most of the nitrous oxide added to the atmosphere each year comes from deforestation and the conversion of forest, savanna and grassland ecosystems into agricultural fields and rangeland. Both of these processes reduce the amount of nitrogen stored in living vegetation and soil through the decomposition of organic matter. Nitrous oxide is also released into the atmosphere when fossil fuels and biomass are burned. However, the combined contribution to the increase of this gas in the atmosphere is thought to be minor. The use of nitrate and ammonium fertilizers to enhance plant growth is another source of nitrous oxide. How much is released from this process has been difficult to quantify. Estimates suggest that the contribution from this source represents from 50% to 0.2% of nitrous oxide added to the atmosphere annually.

Ozone's role in the enhancement of the greenhouse effect has been difficult to determine. Accurate measurements of past long-term (more than 25 years in the past) levels of this gas in the atmosphere are currently unavailable. Moreover, concentrations of ozone gas are found in two different regions of the Earth's atmosphere. The majority of the ozone (about 97%) found in the atmosphere is concentrated in the stratosphere at an altitude of 15 to 55 kilometers above the Earth's surface. This stratospheric ozone provides an important service to life on the Earth as it absorbs harmful ultraviolet radiation. In recent years, levels of stratospheric ozone have been decreasing due to the buildup of human created chlorofluorocarbons in the atmosphere. Since the late 1970s, scientists have noticed the development of severe holes in the ozone layer over Antarctica. Satellite measurements have indicated that the zone from 65° North to 65° South latitude has had a 3% decrease in stratospheric ozone since 1978.

Ozone is also highly concentrated at the Earth's surface in and around cities. Most of this ozone is created as a by product of human created photochemical smog. This buildup of ozone is toxic to organisms living at the Earth's surface.

10.1.3. Atmospheric Structure

Atmospheric layers (figure 10.3) are characterized by variations in temperature resulting primarily from the absorption of solar radiation; visible light at the surface, near ultraviolet radiation in the middle atmosphere, and far ultraviolet radiation in the upper atmosphere.

Troposphere

The troposphere is the atmospheric layer closest to the planet and contains the largest percentage (around 80%) of the mass of the total atmosphere. Temperature and water vapor content in the troposphere decrease rapidly with altitude. Water vapor plays a major role in regulating air temperature because it absorbs solar energy and thermal radiation from the planet's surface. The troposphere contains 99 % of the water vapor in the atmosphere.

All weather phenomena occur within the troposphere, although turbulence may extend into the lower portion of the stratosphere. Troposphere means "region of mixing" and is so named because of vigorous convective air currents within the layer.

The upper boundary of the layer, known as the tropopause, ranges in

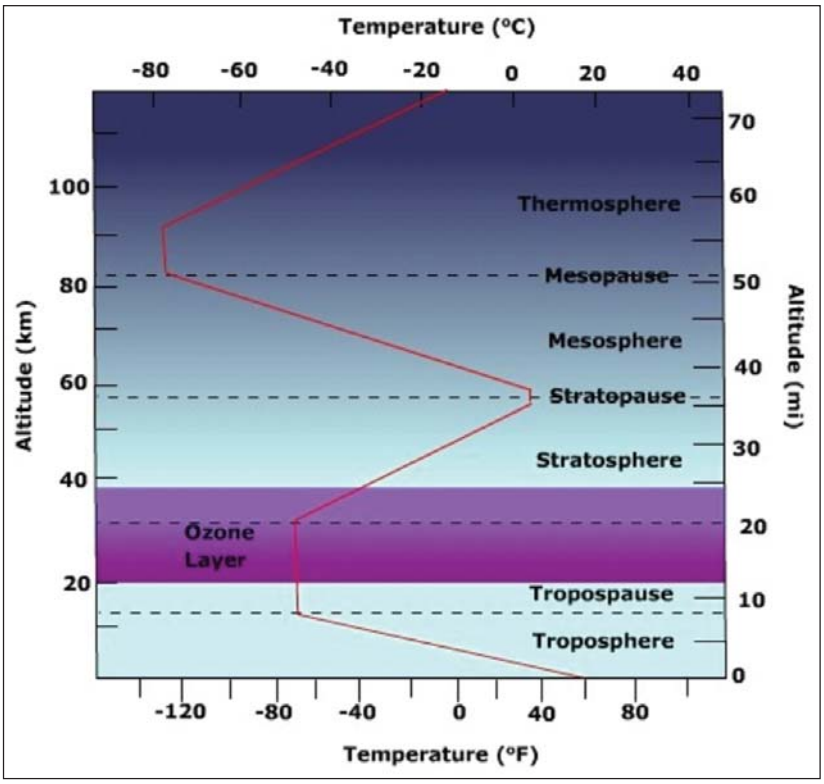

Figure 10.3: Various components of atmosphere (source: http://www.gsfc.nasa.gov/gsfc/service/gallery/fact_sheets/earthsci)

height from 5 miles (8 km) near the poles up to 11 miles (18 km) above the equator. Its height also varies with the seasons; highest in the summer and lowest in the winter.

Stratosphere

The stratosphere is the second major strata of air in the atmosphere. It extends above the tropopause to an altitude of about 30 miles (50 km) above the planet's surface. The air temperature in the stratosphere remains relatively constant up to an altitude of 15 miles (25 km). Then it increases gradually up to the stratopause. Because the air temperature in the stratosphere increases with altitude, it does not cause convection and has a stabilizing effect on atmospheric conditions in the region. Ozone plays the major role in regulating the thermal regime of the stratosphere, as water vapor content within the layer is very low. Temperature increases with ozone concentration. Solar energy is converted to kinetic energy when ozone molecules absorb ultraviolet radiation, resulting in heating of the stratosphere.

The ozone layer is centered at an altitude between 10-15 miles (15-25 km). Approximately 90 % of the ozone in the atmosphere resides in the stratosphere. Ozone concentration in this region is about 10 parts per million by volume (ppmv) as compared to approximately 0.04 ppmv in the troposphere. Ozone absorbs the bulk of solar ultraviolet radiation in wavelengths from 290 nm - 320 nm (UV-B radiation). These wavelengths are harmful to life because they can be absorbed by the nucleic acid in cells. Increased penetration of ultraviolet radiation to the planet's surface would damage plant life and have harmful environmental consequences. Appreciably large amounts of solar ultraviolet radiation would result in a host of biological effects, such as a dramatic increase in cancers.

Mesosphere

The mesosphere, a layer extending from approximately 30 to 50 miles (50 to 85 km) above the surface, is characterized by decreasing temperatures. The coldest temperatures in Earth's atmosphere occur at the top of this layer, the mesopause, especially in the summer near the pole. The mesosphere has sometimes jocularly been referred to as the "ignorosphere" because it had been probably the least studied of the atmospheric layers. The stratosphere and mesosphere together are sometimes referred to as the middle atmosphere.

Thermosphere

The thermosphere is located above the mesosphere. The temperature in the thermosphere generally increases with altitude reaching 600 to 3000 F (600-2000 K) depending on solar activity. This increase in temperature is due to the absorption of intense solar radiation by the limited amount of remaining molecular oxygen. At this extreme altitude gas molecules are widely separated. Above 60 miles (100 km) from Earth's surface the chemical composition of air becomes strongly dependent on altitude and the atmosphere becomes enriched with lighter gases (atomic oxygen, helium and hydrogen). Above about 100 miles (160 km) altitude the major atmospheric component becomes atomic oxygen. At very high altitudes, the residual gases begin to stratify according to molecular mass, because of gravitational separation.

Exosphere

The exosphere is the most distant atmospheric region from Earth's surface. In the exosphere, an upward traveling molecule can escape to space (if it is moving fast enough) or be pulled back to Earth by gravity (if it isn't) with little probability of colliding with another molecule. The altitude of its lower boundary, known as the thermopause or exobase, ranges from about 150 to 300 miles (250-500 km) depending on solar activity. The upper boundary can be defined theoretically by the altitude (about 120,000 miles, half the distance to the Moon) at which the influence of solar radiation pressure on atomic hydrogen velocities exceeds that of the Earth's gravitational pull. The exosphere observable from space as the geocorona is seen to extend to at least 60,000 miles from the surface of the Earth. The exosphere is a transitional zone between Earth's atmosphere and interplanetary space.

10.2. Platforms for measuring atmospheric constituents

Satellites have played an increasingly important role in making remote observations and measurements of global environmental parameters. Satellite motions are governed by the balance between the force of gravity and the centrifugal force due to the satellite's orbital velocity. There are two basic types of meteorological satellites: geostationary and polar orbiting.

Geostationary weather satellites orbit the Earth above the equator at altitudes of 35,880 km (22,300 miles). Because of this orbit, they remain stationary with respect to the rotating Earth and thus can record or transmit images of the entire hemisphere below continuously with their visible-light and infrared sensors. The news media use the geostationary photos in their daily weather presentation as single images or made into movie loops.

Several geostationary meteorological spacecraft are in operation. The United States has two in operation; GOES-11 and GOES-12. GOES-12 is designated GOES-East, over the Amazon River and provides most of the U.S. weather information. GOES-11 is GOES-West over the eastern Pacific Ocean. The Japanese have one in operation; MTSAT-1R over the mid Pacific at 140°E. The Europeans have Meteosat-8 (3.5°W) and Meteosat-9 (0°) over the Atlantic Ocean and have Meteosat-6 (63°E) and Meteosat-7 (57.5°E) over the Indian Ocean. The Russians operate the GOMS over the equator south of Moscow. India also operates geostationary satellites which carry instruments for meteorological purposes. China operates the Feng-Yun geostationary satellites, FY-2C at 105°E and FY-2D at 86.5°E.

Polar orbiting weather satellites circle the Earth at a typical altitude of 850 km (530 miles) in a north to south (or vice versa) path, passing over the poles in their continuous flight. Polar satellites are in sun-synchronous orbits, which means they are able to observe any place on Earth and will view every location twice each day with the same general lighting conditions due to the near-constant local solar time. Polar orbiting weather satellites offer a much better resolution than their geostationary counterparts due to their closeness to the Earth.

Several countries now have satellites in operation (Conway *et al.*, 1997). Russia operates a series of polar orbiting satellites known as Sich / OKEAN (with the Ukraine), the METEOR series, Resors, and MIR -Priroda. Russia also operates a geostationary satellite known as GOMS that transmits infrared images and standard weather maps. China operates the Feng Yun polar orbiter that transmits imagery from both visible and infrared sensors. Japan operates the geostationary meteorological satellite (GMS) which provides visible and infrared images over the western Pacific Ocean, East Asia, and Australia. Japan also has a Marine Observation Satellite (MOS) and, jointly with the US, measures rainfall remotely with the Tropical Rainfall Measuring Mission (TRMM). India operates a geostationary satellite (INSAT) providing distribution of weather maps. The METEOSAT series of geostationary satellites operated by the European Space Agency provide imagery and weather map distribution over Europe and Africa. The Europeans also have the ERS series and ENVISAT. Canada operates RADARSAT, synthetic aperture radar (SAR), which is a powerful microwave instrument that transmits and receives signals to “see” through clouds, haze, smoke, and darkness, and obtain high quality images of the Earth in all weather at any time.

Visible-light images from weather satellites during local daylight hours are easy to interpret even by the average person; clouds, cloud systems such as fronts and tropical storms, lakes, forests, mountains, snow ice, fires, and pollution such as smoke, smog, dust and haze are readily apparent. Even wind can be determined by cloud patterns, alignments and movement from successive photos.

The thermal or infrared images recorded by sensors called scanning radiometers enable a trained analyst to determine cloud heights and types, to calculate land and surface water temperatures, and to locate ocean surface features. These infrared pictures depict ocean eddies or vortices and map currents such as the Gulf stream which are valuable to the shipping industry. Fishermen and farmers are interested in knowing land and water temperatures to protect their crops against frost or increase their catch from the sea. Even El Niño phenomena can be spotted and pollution whether it’s natural or man-made can be pinpointed. The visual and infrared images show the effects of pollution from their respective areas over the entire earth. Aircraft and rocket pollution, as well as condensation trails, can also be spotted. The ocean current and low level wind information gleaned from the space photos can help predict oceanic oil spill coverage and movement.

Almost every summer, sand and dust from the Sahara Desert in Africa drifts across the equatorial regions of the Atlantic Ocean. GOES-EAST images enable meteorologists to observe, track and forecast this sand cloud. In addition to reducing visibilities and causing respiratory problems, sand clouds suppress hurricane formation by modifying the solar radiation balance of the tropics. Other dust storms in Asia and mainland China are common and easy to spot and monitor, with recent examples of dust moving across the Pacific Ocean and reaching North America.

10.3. Remote Sensing of Atmospheric Parameters

The concept of observing system for atmospheric parameters dates back to mid 1960's when planning for combining satellite cloud pictures with radiosondes, aircraft and surface observations were initiated for improved weather forecasting. Satellites have been part of observing system for stratospheric composition related to ozone and its changes for more than 30 years. The new satellite systems can make global observations of key atmospheric constituents in the troposphere. With the advent of new computational and observational capabilities, understanding and predicting global atmospheric composition is becoming more of a reality. Earth system is undergoing rapid changes due to anthropogenic activities. Satellite based observing system is needed to develop understanding of atmospheric composition, the processes that drive the dynamics and to provide the capability to interactions between atmospheric constituents and changes in Earth system due to anthropogenic activities. The observing system for atmospheric composition consists of instruments, models and research. This chapter covers different aspects related to remote sensing of atmospheric constituents such as aerosols, trace gases, temperature, relative humidity and their importance.

The energetic involved in the earth atmosphere system as discussed earlier are shown in Figure10.4. Sun is the natural source of energy and constituents of the earth/atmosphere system reflect/transmit/ absorb the incoming solar energy in different proportions, leading to temperature differences and related dynamics.

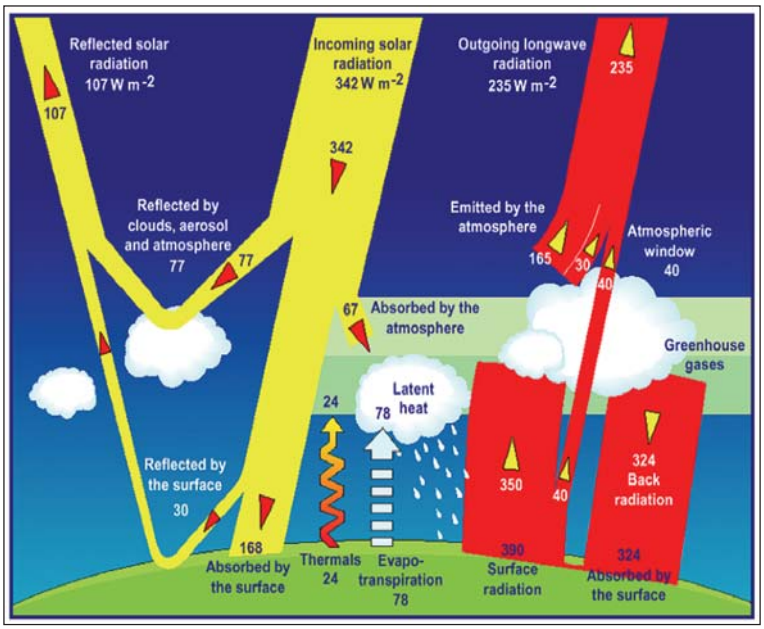

Figure 10.4: Climate system energy balance (source: http://www.gsfc.nasa.gov/gsfc/service/gallery/fact_sheets/earthsci)

The atmospheric constituents determine the air Quality, Earth's radiative balance and the cascading effects such as global warming. The schematic of issues involved in atmospheric composition are shown in Figure 10.5.

Global scale winds move pollutants from one region to another and there is growing awareness that in the Northern Hemisphere, pollution outflow from one continent is reaching the next continent downwind to the east. Thus pollution from the United States gets to Europe; pollution from Europe gets to Asia; and pollution in Asia gets to the United States.

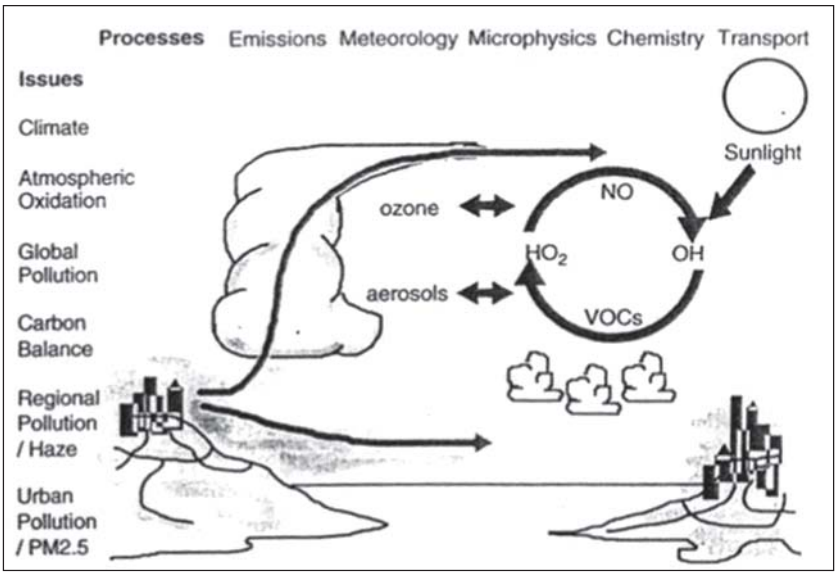

Figure 10.5: Processes and issues related to greenhouse effect (source: http://www.gsfc.nasa.gov/gsfc/service/gallery/fact_sheets/earthsci/green.htm)

Meteorology on all scales influences the atmospheric composition and air quality has become a global issue in recent times. We need to learn how to combine measurements from satellites, ground networks, intensive field campaigns and models on several scales to build an integrated system for creating understanding and predictive capability.

Particulate matter less than 2.5 μm, sulfur dioxide (SO_2), nitrogen dioxide (NO_2), carbon monoxide (CO), aerosols and ozone determine the air quality. There are serious health and environmental effects associated with high concentrations of aerosols and Ozone (O_3). Small size particles can enter the lung causing respiratory problems and enhance the

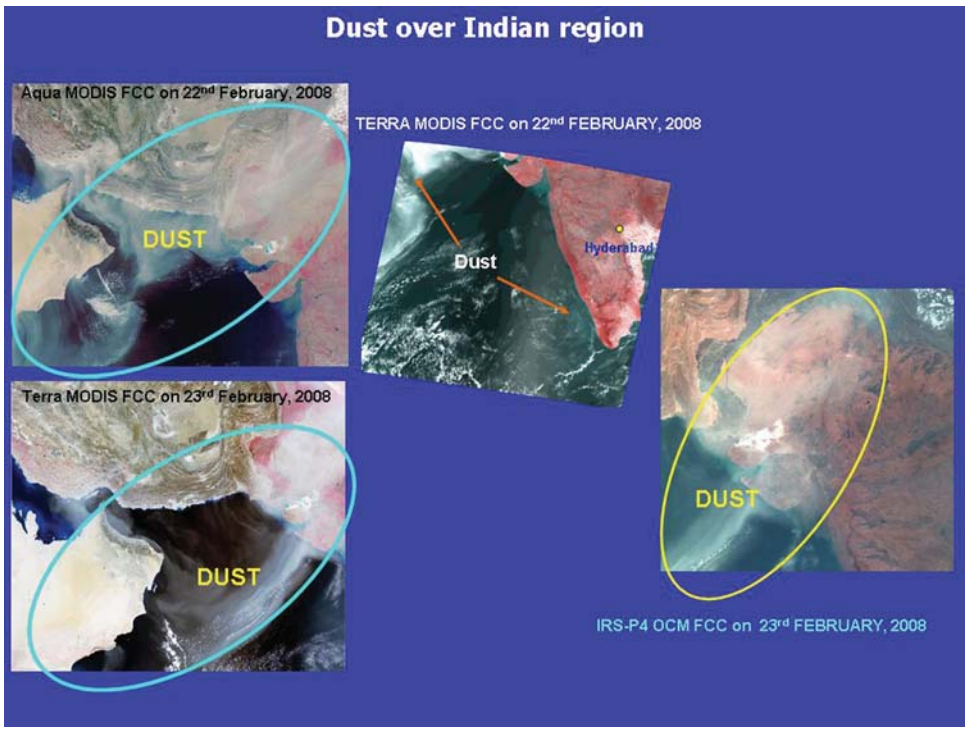

Figure 10.6: Dust storms over Indian region(Badarinath et al., 2010)

concentrations of Ozone, which can affect the immune system and decrease agricultural productivity. It is not possible to control these emissions by reducing the local emission of source gases, such as CO and O_3, as they can be transported to large distances. For example, dust aerosols from Gulf regions is transported over Indian region during pre-monsoon and monsoon period as shown in the TERRA MODIS / IRS-P4 OCM Satellite imagery in Figure 10.6.

The nadir viewing techniques employed by satellite instruments measure the pollutants in the lower troposphere using reflected/scattered sunlight in UV, visible, and near-IR wavelengths (0.3 – 2.5 µm) in figure 10.7. TOMS, GOME and SCIAMACHY are some of the sensors that employ this technique.

10.3.1. Role of aerosols and clouds

Aerosols and clouds tend to counteract the effects of greenhouse gases. Aerosols both absorb and scatter radiation and decrease the energy viable for green house effect. Aerosols are of both natural and anthropogenic origin. Model estimates of radiative forcing of aerosols vary widely between 0 and 2.5 watts/m^2. At the upper limit it is equal to the magnitude but opposite in sign to the greenhouse gas effect of ±2.4watts/m^2. Similarly clouds counteract greenhouse gas effects. Increasing surface temperature increases evaporation from the seas thereby give rise to an increase in cloud cover which can to some extent counteract the greenhouse gas induced global warming. Further the presence of aerosols affects the cloud process. An increase in aerosol content in the atmosphere will increase the cloud forming capacity of the atmosphere which serves as a positive feed back on global warming.

The air quality studies require information on surface concentration and size distribution of aerosols in addition to their vertical distribution and absorptive properties. Atmospheric aerosols are particles of solid or liquid phase dispersed in the atmosphere. These aerosols are produced either by the mechanical disintegration processes occurring over land (such as lifting of dust) and ocean (e.g. sea-spray) or by chemical reactions occurring in the atmosphere. The aerosols at one location are often carried to locations far away from their sources.

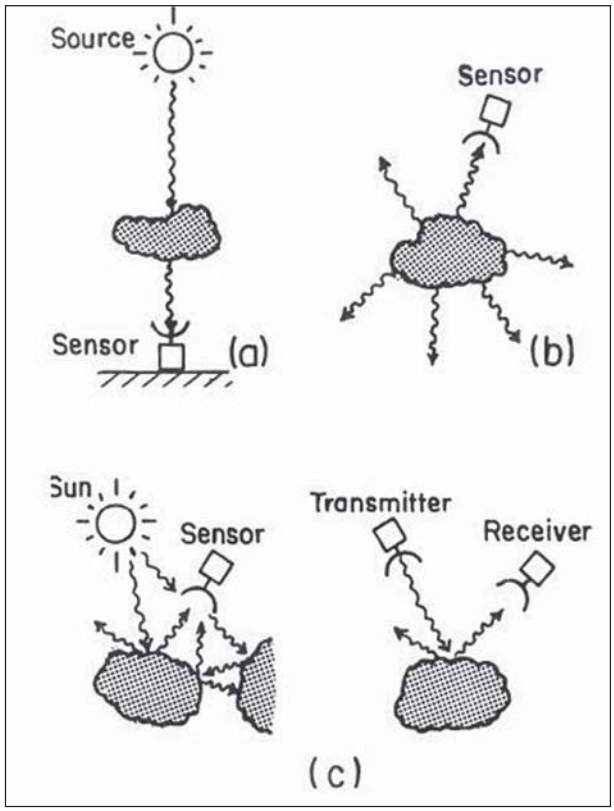

Figure 10.7: Possible receiver / transmitter configurations for remote sensing of atmosphere (source: http: //earthobservatory.nasa.gov/Features/Aerosols/)

Aerosols can vary in size from 10^{-3} to 10^{2} µm depending on the source and production mechanism. Aerosol optical depth (AOD) is quantity which defines the combined effect of scattering and absorption in a vertical column of atmosphere. The optical depth due to aerosols, i.e., "Aerosol Optical Depth (AOD)" is obtained by subtracting the contribution due to air molecules from total optical depth. AOD (t) is derived from the satellite measurement of top of the atmosphere reflectance (TOA) in the visible wavelength bands. The method for estimating aerosol optical depth is described below.

10.3.2. Physical principles of aerosol retrieval from space

One component of the satellite-observed radiance carries information about aerosol, and this component can be isolated as.

$$L(\mu, \varphi) = L_o(\mu, \varphi) + \frac{a}{1 - aR_s} \mu_0, F_0 T\, d(\mu_0) T_u(\mu)$$

For isotropic surface reflection the satellite observed L, after separation of Rayleigh and gaseous components, the same equation holds for aerosol alone. For $\tau < 1$, in single- scattering approximation L_0 is:

$$L_0(\mu, \varphi) \approx \frac{F_0}{4\mu} \omega P(\mu, \varphi, -\mu_0, \varphi_0)\tau$$

Where,

L = satellite observed radiance; L_0 = Atmospheric path radiance; T_d = Total transmittance for downward radiation; T_u = Total transmittance for upward radiation; R_s = Spherical reflectance of atmosphere; a = Surface albedo; F_0 = Normal solar irradiance at TOA; μ_0 = Cosine of solar zenith angle; µ, φ = Cosine of view angle and relative azimuth angle; τ = Optical thickness; ρ = Scattering phase function; ω = Single scattering albedo

The Moderate Resolution Imaging Spectrometer (MODIS) aboard EOS Terra and Aqua satellites makes multi - spectral measurements of top of the atmosphere reflectance (r) to determine the size distribution of aerosols in fine or coarse mode. This helps in the determination of aerosol scattering phase function, "P". Figure 10.8 shows the MODIS derived aerosol optical depth on two dates over Indian region. The increased values of aerosol optical depth over Indo-Gangetic Plains can be observed in the Figure 10.8. The accuracy of MODIS AOD over land regions is not good due to heterogeneity in land surface reflectance. Recently, a new algorithm, called the "deep blue" algorithm has been developed to improve the estimation over land. This algorithm uses the 412 and 419 nm MODIS channels, where the land is darker at the longer wavelengths.

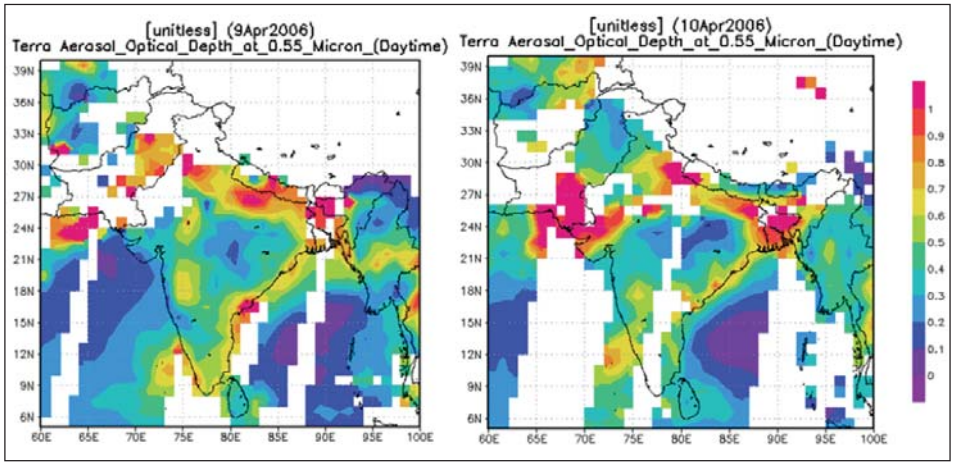

Figure 10.8: TERRA MODIS derived aerosol optical depth(Badarinath et al., 2007)

In addition to satellite based estimation of AOD in visible region of the electromagnetic spectrum (EMR), methods exist to estimate aerosol absorption optical depth t_a using ultraviolet wavelengths. Aerosol index (AI), a measure of the absorbing aerosol concentration in atmosphere, is regularly estimated from 1978, using Total Ozone Monitoring Instrument (TOMS) on board Earth Probe (EP) and was recently replaced by AURA-OMI. In the ultraviolet wavelengths, land is opaque, and the wavelength of top of the atmosphere reflectance provides information on the absorbing aerosols in the atmosphere. It is possible to make quantitative estimates of t_a and t_s from measurements of top of atmosphere reflectance (ñ) at two ultraviolet wavelengths (Torres *et al.*, 1998). By combining the deep blue, visible and the UV methods, estimation of both the scattering and absorption optical depths of aerosols over

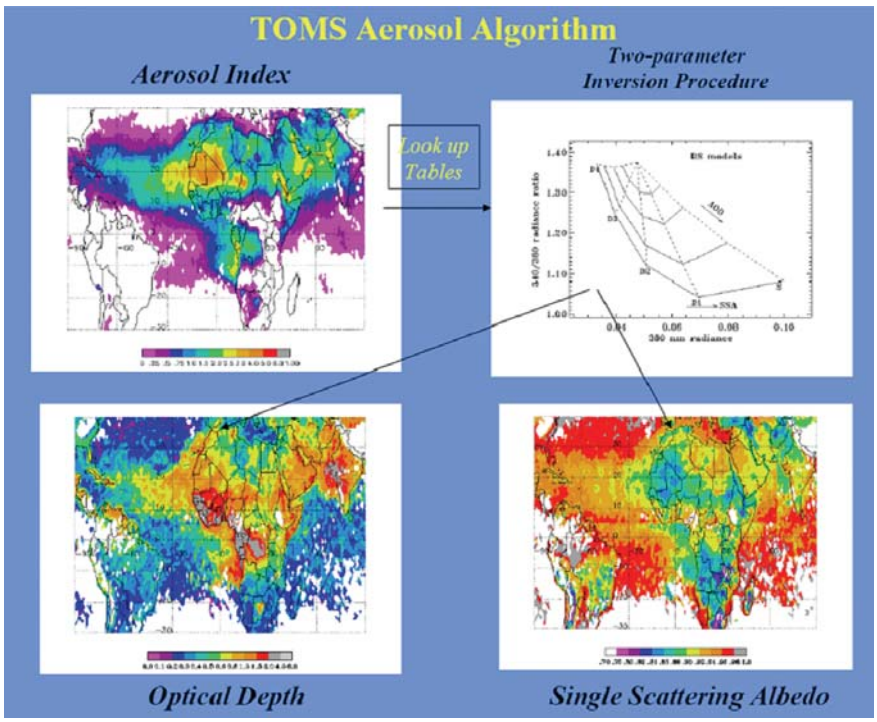

Figure 10.9: TOMS Aerosol algorithm(Torres et al., 1998)

land and ocean can be made (figure 10.9).

Estimation of tropospheric Ozone (O_3) remains a challenge for satellite measurements, as radiation sensitive to tropospheric ozone has to pass through the stratosphere before reaching to the satellite. The satellite measurements are so far able to achieve estimation of tropospheric ozone from total columnar ozone by subtracting the stratosphere overburden. There are several methods available, including the use of limb viewing instruments, such as Microwave Limb Sounder (MLS) and The Stratospheric Aerosol and Gas Experiment (SAGE) that can measure down to the tropopause to estimate stratospheric Ozone overburden.

Nitrogen Dioxide (NO_2) is a byproduct of combustion produced by automobiles and biomass burning besides it is also produced by lightning. Scanning Imaging Absorption Spectrometer for Atmospheric Cartography (SCIAMACHY) onboard ENVISAT satellite makes measurement of NO_2. Since NO_2 occurs mostly in the planetary boundary layer, the accuracy of these products requires careful scrutiny.

10.3.3. Physical basis of TOMS aerosol retrieval approach

Neglecting particle multiple scattering effects, the upwelling reflectance as measured by a satellite, is approximately given by:

Since I_0 depends on pressure, then

Aerosol single scattering contribution

Attenuation of Rayleigh and surface components by aerosol absorption

$$I \approx \frac{\omega_0 P(\Theta)\pi F}{4\pi} \frac{\mu_0}{\mu_0+\mu}\left[1-e^{-\tau(1/\mu+1/\mu_0)}\right]+[I_s+I_0]e^{-(1-\omega_0)\tau(1/\mu+1/\mu_0)}$$

$$I \approx \frac{\omega_0 P(\Theta)\pi F_0}{4\pi} \frac{\mu_0}{\mu_0+\mu}\left[1-e^{-\tau(1/\mu+1\mu_0)}\right]+\left[\frac{(\rho_s \rho_a) I_0}{\rho_s}+I_s\right]e^{-(1-\omega_0)\tau(1/\mu+1/\mu_0)}+\frac{\rho_a}{\rho_s}+I_s$$

ρ_s and ρ_a are surface and aerosol layer height pressure levels. The net aerosol contribution to the measured reflectance is-

Where,

πF_0 = Solar flux; ω_0 = Single scattering albedo; τ = Aerosol optical depth; μ, μ_0 = Cosines of satellite and solar zenith angles; b (Θ) = Aerosol scattering phase function,

The principle used for measuring carbon monoxide (CO) employs 2.3 µm absorption bands, where there is still a sufficient amount of sunlight to measure the reflected radiation. Satellite measurement of CO mainly comes from

the 4.6 µm thermal emission band, which provides CO in the middle troposphere. Recent results have come out from the MOPITT instrument onboard EOS Terra and the AIRS instrument onboard EOS Aqua satellite. Sulfur Dioxide (SO_2) mainly comes from both natural sources such as fuming volcanoes and anthropogenic sources such as burning of sulfur rich coal. Satellite base instruments such as GOME, SCIAMACHY and OMI with spectral bands in UV region provide global maps of SO_2 (Figure10.10a & 10b).

Sensor	TOMS/ TRIANA	AVHRR/ SEAWIFS	GOME	MOPITT	MODIS	SCIA MACHY	MIPAS	SAGE III	TES	HRDLS	OMI	MLS
Launch	1979		1995	1999	1999	2002	2002	2004	2004	2004	2004	2004
O_3	col		col			col/limb	limb	limb	nadir/limb	limb	col	limb
H_2O	col					col/limb	limb	limb	nadir/limb	limb		limb
CO				nadir		col/limb	limb		nadir/limb			limb
NO									limb			
NO_2			col			col/limb					col	
HNO_3							limb		limb	limb		
CH_4				col		col/limb			col	limb		
CH_2O			col			col/limb					col	
SO_2						col			col		col	
CO_2						col/limb						
BrO			col			col					col	
HCN												limb
Aerosol	col	col			col	col/limb		limb		limb	col	

Figure 10.10a: Present Satellite Measurements for Tropospheric Chemistry (source: www.esa.int)

Precipitation is one of the most variable quantities in space and time. Precipitation also has a direct impact on human life that other atmospheric phenomena seldom have: an example is represented by heavy rain events and flash floods.

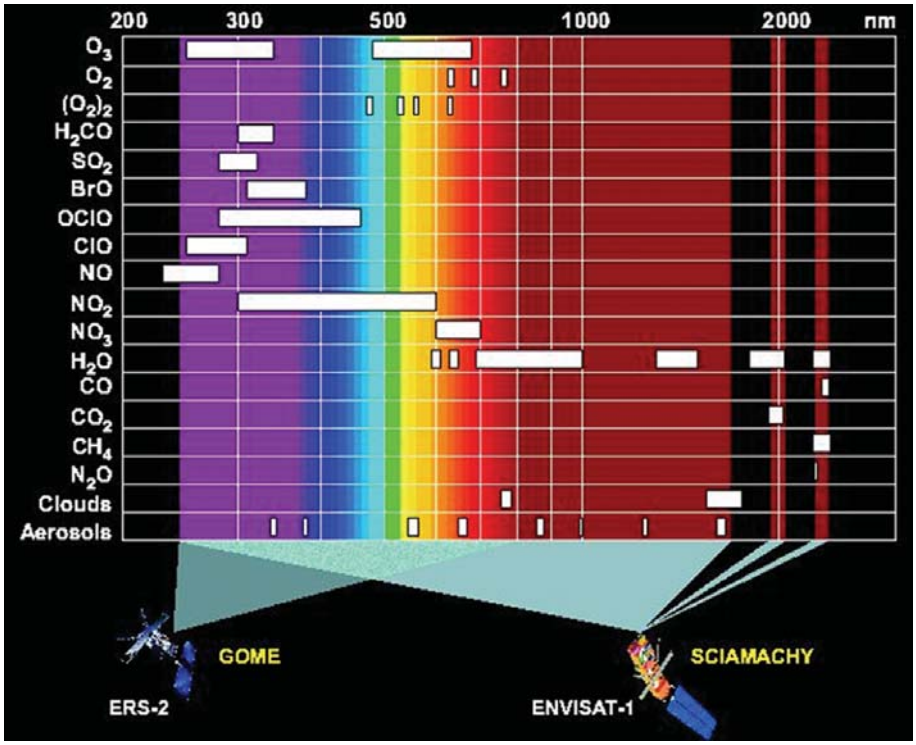

Figure 10.10b: Different spectral bands used in Satellite observation of trance gases and aerosols (source: www.esa.int)

Satellite remote sensing is an efficient tool for measuring rainfall on various spatial and temporal scales that has many applications in meteorology, hydrology and climate studies. Over India and adjoining oceans, the reliable ground based radars and dense network of rain gauge information is available but only for limited areas. Although geostationary satellite IR measurements benefit from high temporal sampling, IR radiances from cloud tops have only an indirect relationship with surface rainfall which so far resulted in weak statistical relationships between rainfall and cloudiness. The most common GOES Precipitation Index (GPI) technique (Arkin and Meisner 1987) based on simple IR-TB threshold algorithm have been in operation to produce tropical and subtropical precipitation products for various climatological studies (Arkin and Xie 1994). Satellite microwave measurements on the other hand have a very good physical connection with the rain and hydrometeors. There are many satellite microwave based techniques for rainfall estimation over land and oceans (Ferraro and Marks 1995, Wilheit *et al.*, 2003, Kummerow *et al.*, 1996, Liu and Curry 1992).

Rainfall estimation from IR and visible observations from geostationary and low orbiting satellites basically depends on combining multi-spectral measurements to estimate precipitation. One of the principal innovations of these

methods relative to earlier simpler temperature threshold based algorithms is that, it optimally combines several cloud properties used in a variety of techniques in a single and comprehensive rainfall algorithms. For example, the GOES Multi-Spectral Rainfall Algorithm (GMSRA) (Ba and Gruber 2001), Hydro-Estimator (H-E) (Scofield and Kuligowski 2003.) techniques from NOAA uses many such cloud property in VIS and IR regions. The GMSRA uses the cloud top temperature as a basis of rain estimation (e.g., Arkin and Meisner; 1987, Ba *et al.*, 1995; Vicente *et al.*, 1998) and utilizes the effective radii of cloud particles, i.e., the cloud microphysics (e.g., Rosenfield and Gutman 1994) and spatial and temporal gradients (e.g., Adler and Negri 1988; Vicente *et al.*, 1998) to screen out non-raining clouds and humidity.

The development of hybrid techniques using the strengths of both microwave and IR is highly desirable based on their proper inter-calibration over the common areas of overlap. One such algorithm was developed by Vicente *et al.*, (1998) called auto-estimator, using GOES (IR) and surface microwave radar-rainfall. Adler *et al.* (1994) developed a technique called Adjusted GPI (AGPI) in which a correction factor is derived from the comparison of passive microwave and GPI estimates for coincident time slots (from 3 hourly to one month). Gairola *et al.*, 2004; Gairola and Krishnamurthy 1992; Joyce *et al.*, 2004 developed techniques in which the IR channel is used as a means to spatially and temporally transport the rainfall features in conjunction with satellite passive microwave observations.

The inherent limitations of optical channels remain persistent for rainfall retrieval as the rainfall in the ground is inferred by cloud top signatures only. There is no direct physical connection between the rain/cloud and ice hydrometeors within the clouds with radiance emanating from cloud tops to the sensor. The accuracy of rainfall estimate improves marginally even with significant new efforts. However, the high spatial and temporal coverage of geostationary optical measurements is the very strong point along with the resolution capabilities of the sensors. At the same time microwaves have direct physical connections with vertical structure of rainfall and thus with the cloud, rain and ice hydrometeors. But the non-portability of microwave sensors to the geostationary platforms till date due to technological constraints is a limitation and thus only low earth orbiting satellites can provide the rainfall information for land, ocean and atmosphere. With the advent of active and passive radar and radiometric sensors onboard a single satellite (e.g., Tropical Rainfall Measuring Mission-TRMM) we envisage that a technique like GMSRA can be further improved for Indian tropical regions and more reliable rainfall information can be retrieved. We henceforth call this technique as INSAT Multispectral Rainfall Algorithm (IMSRA), as a specific technique for Indian Tropical regions. Our objectives for both the techniques (GPI and IMSRA) here are based on these premises and are outlined below (mainly in cases of IMSRA).

King (1956) was first to suggest that atmospheric temperature profiles could be inferred from satellite observations of thermal infrared emission and explained the feasibility of retrieving the temperature profile from the satellite intensity scan measurements. Further advances were made for the temperature sounding concept by Kaplan (1959) demonstrated that vertical profile of temperature could be inferred from the spectral distribution of emission by atmospheric gases. He suggested that observations in the wings of a spectral band sense deeper regions of the atmosphere, whereas observations in the band center see only the very top layer of the atmosphere, since the radiation mean free path is small. Thus by properly selecting a set of sounding spectral channels at different wavelengths in the absorption band, the observed radiances could be used to estimate the vertical temperature profile in the atmosphere.

Following a proposal by Wark (1961) for satellite vertical sounding program to measure atmospheric temperature profiles, the first satellite with sounding instrument (SIRS-A) was launched on NIMBUS-3 in 1969 (Wark *et al.*, 1970). NOAA launched the TIROS Operational Vertical Sounder in 1978 (TOVS, Smith *et al.* 1979), consisting of High resolution Infrared Radiation Sounder (HIRS), Microwave Sounding Unit (MSU), and the Stratospheric Sounding Unit (SSU) onboard satellites NOAA-6 to NOAA-14. HIRS provides 17 km spatial resolution at nadir with 19 infrared sounding channels (4-15 μm), whereas MSU provides 109 km resolution at nadir with 4 microwave channels (~50 GHz). SSU has 3 channels in the far IR (~15 μm) for stratospheric measurements. Current NOAA series satellites NOAA-15 and NOAA-16 (and future satellite in the NOAA series) have ATOVS with HIRS/3, and MSU and SSU have been replaced by AMSU-A and AMSU-B to improve the temperature and humidity sounding. HIRS/3 has the same spectral bands as the HIRS/2. AMSU-A uses 15 microwave channels around 23, 30, 50 and 90 GHz of oxygen absorption bands with resolution of 50 km at nadir. AMSU-B uses 5 microwave channels around 90, 150 and 190 GHz with a horizontal resolution of 17 km at nadir.

New generation of infrared atmospheric sounders are hyper-spectral sounder with thousands of channels instead of few tens of infrared bands. Atmospheric Infra-Red Sounder (AIRS) onboard EOS-Aqua satellite was launched on May 4, 2002 providing a wealth of highly accurate atmospheric and surface information using 2378 high spectral-

resolution infrared (3.7 – 15.4 µm) channels with horizontal resolution of 10 km at nadir. AIRS along with AMSU forms a state-of-art atmospheric sounding tool for temperature profiles with accuracy of 1° C in a 1 km thick layer and humidity profile with an accuracy of 20% in 2 km thick layer in the troposphere. Aqua satellite also has MODIS with very high spatial resolution of 1 km and is providing the vertical profiles of temperature and humidity. Recently, METOP satellite was launched carrying a hyper spectral sounder IASI onboard with >8400 channels and mission objectives were to achieve the temperature and humidity profiles accuracy of 1° C and 10% in 1 km and 2km layers, respectively. The first sounding instrument in geostationary orbit was the GOES VISSR Atmospheric Sounder (VAS, Smith *et al.* 1981) launched in 1980. This was followed by GOES-8 Sounder (Menzel and Purdom, 1994) that provides 8 km spatial resolution with 18 infrared sounding channels. Current satellite of this series, GOES-13, was launched recently in May 2006. Future satellite of this series GOES-R is to be launched in 2012 and it will have a Hyperspectral Environmental Suite (HES) to provide high spectral resolution in the infrared and a high spatial resolution mode for mesoscale sounding capability. Advanced Baseline Imager (ABI) onboard GOES-R will be similar to the current polar orbiting EOS-MODIS. NASA and NOAA are planning to launch Geostationary Imaging Fourier Transform Spectrometer (GIFTS) that will revolutionize our ability to measure, understand and predict the earth-atmosphere system. India is planning to launch a meteorological satellite INSAT-3D in geostationary orbit towards the end of 2010. INSAT-3D will carry an 18-channel infrared Sounder (in addition to visible channel) along with a 6 channel Imager. The algorithm for retrieving vertical profiles of atmospheric temperature and moisture along with ozone from INSAT-3D Sounder observations of clear sky infrared radiances in different absorption bands. INSAT-3D Sounder channels are similar to those in GOES-12 Sounder and many of the spectral bands are similar to High resolution Infrared Radiation Sounder (HIRS) onboard NOAA- ATOVS. Observations in these Sounder channels can be used to retrieve profiles of temperature and moisture as well as total column estimates of ozone. INSAT-3D Sounder observations will provide vertical profiles of temperature and humidity in clear-sky conditions besides total column ozone and various other derived products.

Atmospheric profile retrieval algorithm for INSAT-3D Sounder is a two-step approach. The first step includes generation of accurate hybrid first guess profiles using combination of statistical regression retrieved profiles and model forecast profiles. The second step is nonlinear physical retrieval to improve the resulting first guess profile using Newtonian iterative method. The retrievals will be performed using clear sky radiances measured by Sounder within a 5x5 field of view (approximately 50 km resolution) over land and ocean for both day and night. Separate regression coefficients will be generated for land and ocean for day and night conditions using a training dataset comprising historical radiosonde observations representing atmospheric conditions over INSAT-3D observation region. INSAT-3D Sounder has 18 infrared channel and a visible channel to help cloud detection during daytime. The normal mode of Sounder operation covers 6000km x 6000km field of view and takes approximately 160 minutes. In addition, the instrument is designed with flexible modes of operation for fast and repetitive coverage.

INSAT- 3D Sounder retrieval scheme involves two-step approach, with first step as regression retrieval combined with model forecast to prepare the temperature and humidity profile, followed by the second step as physical retrieval procedure that uses non-linear Newtonian iterative method to adjust the first guess to obtain accurate retrieval of temperature, and humidity profile. Ozone profile and integrated amount is retrieved using regression retrieval and used as first guess for the physical retrieval routine. Atmospheric sounding is one of the most important applications of satellite measurements in meteorology, which involves retrieving vertical profiles of temperature and trace-gas concentrations, especially water vapor and ozone. This is done by making observations at wavelengths that have significant attenuation in atmosphere (figure 10.11 and 12). For this we need to know the variation of temperature with altitude, and the variation of the density of atmospheric gases with altitude, such as carbon-dioxide, water vapour and ozone. Water vapor is important because of its

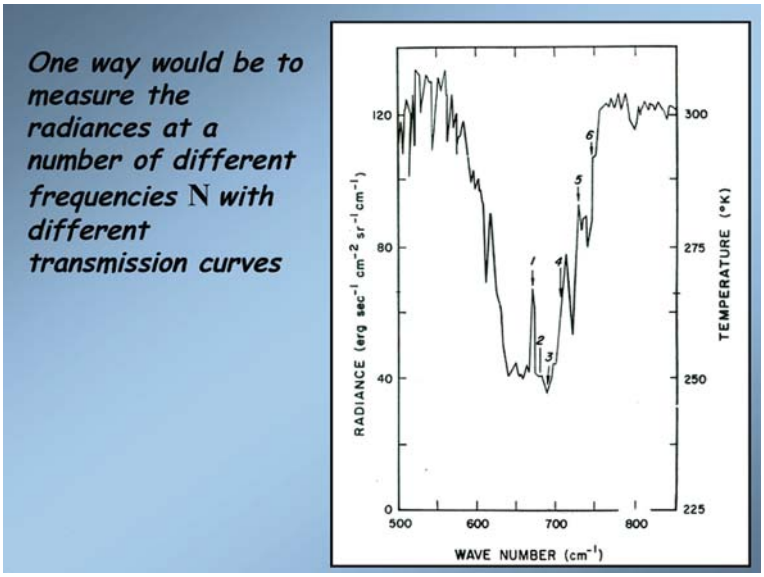

Figure 10.11: Atmospheric sounding of atmosphere at different wavelengths for deriving temperature (source: http: // earthobservatory.nasa.gov/Features/Aerosols/)

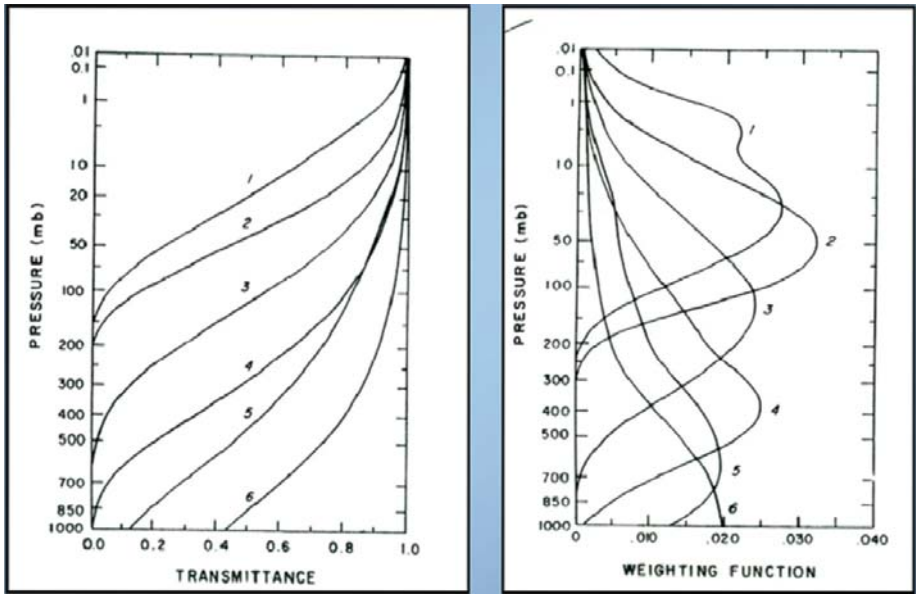

Figure 10.12: Transmission and weighting functions (source: http://www.ua.nws.noaa.gov/factsheet.htm)

meteorological impact and its importance for atmospheric correction in thermal infrared measure-ments.

Atmospheric sounding techniques exploit all three phenomena that play important role in radiative transfer processes: namely absorption, scattering and thermal emission. Most observations are made in the thermal infrared and microwave bands. At infrared wavelengths scattering due to atmospheric gases is negligible, and is not considered in the radiative transfer process. For nadir IR earth radiance methods the RT problem is more complicated and non-linear.

The upwelling 'Earth' radiance at wavelength l, or frequency (wave number) õ, observed looking down, is given by:

$$\tau_{\nu}(a,b) = \exp\left(-\int_{z=a}^{z=b} n(z)\sigma_{\nu} dz\right)$$

$$L_{\nu}(Z^{*}) = \varepsilon_{surf} B_{\nu}(T_{surf})\tau_{\nu}(0,Z^{*}) + \int_{z=0}^{z^{*}} B_{\nu}(T_{z})\, n(Z)\sigma_{\nu}\tau_{\nu}(Z,Z^{*})\, dz$$

$$L_{\nu}(Z^{*}) = \varepsilon_{surf} B_{\nu}(T_{surf})\tau_{\nu}(0,Z^{*}) + \int_{z=0}^{z^{*}} B_{\nu}(T_{z})[\, d\tau_{\nu}(Z,Z^{*})/dZ\,]\, dZ$$

For vertical sounding theory at infrared wavelengths, the significant terms in the radiative transfer equation (RTE) are absorption and thermal emission. This simplification is called Schwartzchild's equation. Here, we consider only cloud-free conditions. If a sensor views vertically downwards into the atmosphere at a wavelength at which the atmosphere is optically thick, the brightness temperature/radiances that is received by sensor will be characteristic of the atmosphere at a depth below the sensor that is of the order of the absorption length. Thus, the greater the absorption coefficient, the smaller the absorption length, and hence the greater the altitude from which the temperature signal is received. So by making observations at a number of wavelengths near a broad absorption line, different altitudes in the atmosphere can be investigated. Thermal infrared temperature profilers normally employ the broad and deep CO_2 lines near 15 µm wavelengths.

10.4. Present and Future Missions

10.4.1. INSAT Series

INSAT or the Indian National Satellite System is a series of multipurpose geo-Stationary satellites launched by ISRO for the telecommunications, broadcasting, meteorology, and "search and rescue" needs of India. Commissioned in 1983, INSAT is the largest domestic communication system in the Asia-Pacific Region. It is a joint venture of the Department of Space, Department of Telecommunications, India Meteorological Department, All India Radio and Doordarshan. The overall coordination and management of INSAT system rests with the Secretary-level INSAT Coordination Committee.

INSAT satellites provide 199 transponders in various bands (C, S, Extended C and Ku) to serve the television and communication needs of India. Some of the satellites of the INSAT series also carry the Very High Resolution Radiometer (VHRR), CCD cameras for meterological imaging. The satellites also incorporate transponders for receiving distress alert signals for search and rescue missions in the South Asian and Indian Ocean Region, as ISRO is a member of the Cospas-Sarsat programme.

INSAT system

The Indian National Satellite (INSAT) system was commissioned with the launch of INSAT-1B in August 1983 (INSAT-1A), the first satellite was launched in April 1982 but could not fulfill the mission. INSAT system ushered in a revolution in India's television and radio broadcasting, telecommunications and meteorological sectors. It enabled the rapid expansion of TV and modern telecommunication facilities to even the remote areas and off-shore islands. Today, INSAT has become the largest domestic communication satellite system in the Asia-Pacific region with ten satellites in service - INSAT-2E, INSAT-3A, INSAT-3B, INSAT-3C, INSAT-3E, KALPANA-1, GSAT-2, EDUSAT, INSAT-4A and INSAT-4B (table 10.2). Together, the system provides 199 transponders in C, Extended C and Ku bands for a variety of communication services. Some of the INSATs also carry instruments for meteorological observations and data relay for providing meteorological services. KALPANA-1 is an exclusive meteorological satellite. The satellites are monitored and controlled by Master Control Facilities that exist in Hassan and Bhopal.

Satellites in service

There are currently 11 satellites in service out of 21 which have ever been part of INSAT system.

Table 10.2: INSAT satellites

Sl. No.	Satellite	Launch Date	Mission Status
1	INSAT-1A	10 April 1982	Deactivated on 6 September 1982
2	INSAT-1B	30 August 1983	Completed mission life
3	INSAT-1C	22 July 1988	Abandoned in November 1989
4	INSAT-1D	12 June 1990	Completed mission life
5	INSAT-2A	10 July 1992	India's First Indegenious communication Satellite. Completed mission life
6	INSAT-2B	23 July 1993	Completed mission life
7	INSAT-2C	7 December 1997	Completed mission life
8	INSAT-2D	4 June 1997	Became inoperable on 4 October 1997
9	INSAT-2DT	In-orbit procurement	Completed mission life
10	INSAT-2E	3 April 1999	In service
11	INSAT-3A	10 April 2003	In service
12	INSAT-3B	22 May 2000	In service
13	INSAT-3C	24 January 2002	In service
14	KALPANA-1	12 September 2002	In service
15	GSAT-2	8 May 2003	In service
16	INSAT-3E	28 September 2003	In service
17	EDUSAT	20 September 2004	In service
18	INSAT-4A	22 December 2005	In service
19	INSAT-4B	12 March 2007	In service
20	INSAT-4CR	2 September 2007	in geo-synchronous orbit

INSAT-2E

It is the last of the five satellites in INSAT-2 series. It carries seventeen C-band and lower extended C-band transponders providing zonal and global coverage with an Effective Isotropic Radiated Power (EIRP) of 36 dBW. It also carries a Very High Resolution Radiometer (VHRR) with imaging capacity in the visible (0.55-0.75 µm), thermal infrared (10.5-12.5 µm) and water vapour (5.7-7.1 µm) channels and provides 2x2 km, 8x8 km and 8x8 km ground resolution, respectively. In addition to the above two payloads it has with it a Charge Coupled Device (CCD) camera providing 1x1 km ground resolution in the Visible (0.63-0.69 µm), Near Infrared (0.77-0.86 µm) and Shortwave Infrared (1.55-1.70 µm) bands.

INSAT-3 Series

INSAT-3A

The multipurpose satellite, INSAT-3A, was launched by Ariane in April 2003. It is located at 93.5 degree East longitude. The payloads on INSAT-3A are as follows:

- 12 Normal C-band transponders (9 channels provide expanded coverage from Middle East to South East Asia with an EIRP of 38 dBW, 3 channels provide India coverage with an EIRP of 36 dBW and 6 Extended C-band transponders provide India coverage with an EIRP of 36 dBW)
- 6 Ku-band transponders provide India coverage with EIRP of 48 dBW
- A Very High Resolution Radiometer (VHRR) with imaging capacity in the visible (0.55-0.75 µm), thermal infrared (10.5-12.5 µm) and Water Vapour (5.7-7.1 µm) channels, provide 2x2 km, 8x8 km and 8x8 km ground resolutions respectively
- A CCD camera provides 1x1 km ground resolution, in the visible (0.63-0.69 µm), near infrared (0.77-0.86 µm) and shortwave infrared (1.55-1.70 µm) bands
- A Data Relay Transponder (DRT) having global receive coverage with a 400 MHz uplink and 4500 MHz downlink for relay of meteorological, hydrological and oceanographic data from unattended land and ocean-based automatic data collection-cum-transmission platforms
- A Satellite Aided Search and Rescue (SAS&R) SARP payload having global receive coverage with 406 MHz uplink and 4500 MHz downlink with India coverage, for relay of signals from distress beacons in sea, air or land.

INSAT-3B

Launched in March 2000, INSAT-3B is collocated with INSAT-2E at 83 degree East longitude. It carries 12 Extended C-band transponders and three Ku-band transponders that have coverage over the Indian region. INSAT-3B also incorporates a Mobile Satellite Services (MSS) payload with forward link between the hub and mobile station operating in CxS band and return link between the mobile station and the hub operating in SxC band.

INSAT-3C

Launched in January 2002, INSAT-3C is positioned at 74 degree East longitude. INSAT-3C payloads include 24 Normal C-band transponders providing an EIRP of 37 dBW, six Extended C-band transponders with EIRP of 37 dBW, two S-band transponders to provide BSS services with 42 dBW EIRP and an MSS payload similar to that on INSAT-3B. All the transponders provide coverage over India.

INSAT-3E

Launched in September 2003, INSAT-3E is positioned at 55 degree East longitude and carries 24 Normal C-band transponders provide an edge of coverage EIRP of 37 dBW over India and 12 Extended C-band transponders provide an edge of coverage EIRP of 38 dBW over India.

KALPANA-1

KALPANA-1 is an exclusive meteorological satellite launched by PSLV in September 2002. It carries VHRR and DRT payloads to provide meteorological services. It is located at 74 degree East longitude.

GSAT-2

Launched by the second flight of GSLV in May 2003, GSAT-2 is located at 48 degree East longitude and carries four Normal C-band transponders to provide 36 dBW EIRP with India coverage, two Ku-band transponders with 42 dBW EIRP over India and an MSS payload similar to those on INSAT-3B and INSAT-3C.

EDUSAT

Configured for audio-visual medium employing digital interactive classroom lessons and multimedia content, EDUSAT was launched by GSLV in September 2004. Its transponders and their ground coverage are specially configured to cater to the educational requirements. The satellite carries a Ku-band transponder covering the Indian mainland region with 50 dBW EIRP, five Ku-band spot beam transponders for South, West, Central, North and North East regional coverage with 55 dBW EIRP and six Extended C-band transponders with India coverage with 37 dBW EIRP. EDUSAT is positioned at 74 degree East longitude and is collocated with KALPANA-1 and INSAT-3.

INSAT-4 Series

INSAT-4A

Launched in December 2005 by the European Ariane launch vehicle, INSAT-4A is positioned at 83 degree East longitude along with INSAT-2E and INSAT-3B. It carries 12 Ku-band 36 MHz bandwidth transponders employing 140 W TWTAs to provide an EIRP of 52 dBW at the edge of coverage polygon with footprint covering Indian main land and 12 C-band 36 MHz bandwidth transponders provide an EIRP of 39 dBW at the edge of coverage with expanded radiation patterns encompassing Indian geographical boundary, area beyond India in southeast and northwest regions. Tata Sky, a joint venture between the TATA Group and Star uses INSAT-4A for distributing their Direct To Home Digital Television services across India.

INSAT-4B

It was launched in March 2007 by the European Ariane launch vehicle. Configured with payloads identical to that of INSAT-4A, INSAT-4B carries 12 Ku-band and 12 C-band transponders to provide EIRP of 52 dBW and 39 dBW respectively. Two Tx/Rx dual grid offset fed shaped beam reflectors of 2.2 m diameter for Ku-band and 2 m diameter for C-band are used. INSAT-4B augments the high power transponder capacity over India in Ku-band and over a wider region in C-band. It is co-located with INSAT-3A at 93.5 degree E longitude.

INSAT-4CR

INSAT-4CR was launched on 2 September 2007 by GSLV-F04. It carries 12 Ku-band 36 MHz bandwidth transponders employing 140 W TWTAs to provide an Effective Isotropic Radiated Power of 51.5 dBW at Edge of Coverage with footprint covering Indian mainland. It also incorporates a Ku-band Beacon as an aid to tracking the satellite. The satellite is designed for a mission life in excess of ten years.

In addition to measurements of atmospheric constituents, satellite data from polar orbiting and geostationary satellites are been used to understand cloud properties, vertical profiles of temperature, humidity etc. In the Indian context, data from INSAT series are being used to study winds, OLR, water vapour etc. India is planning to launch a meteorological satellite INSAT-3D in geostationary orbit towards the end of 2010. INSAT-3D will carry an 18-channel infrared Sounder (plus a visible channel) along

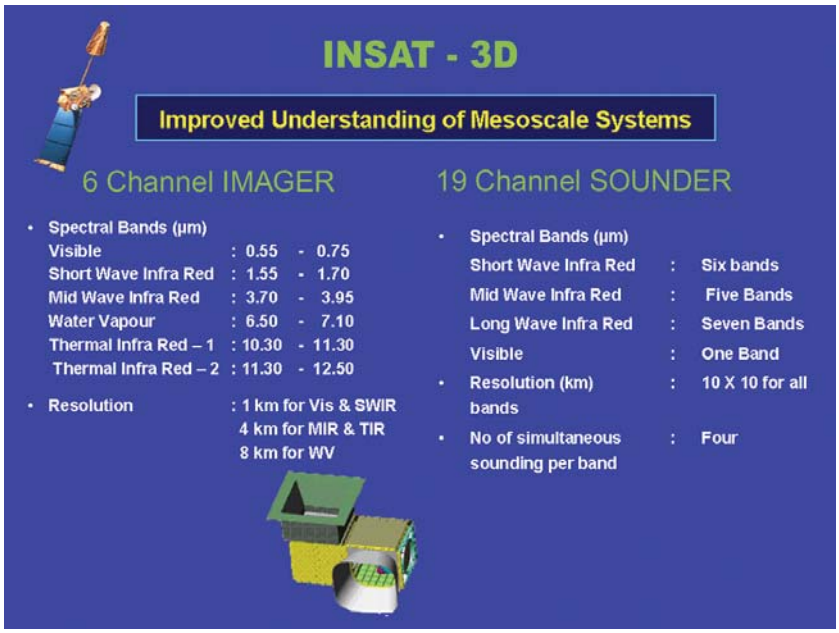

Figure 10.13: Characteristics of INSAT-3D sensors (source: www.isro.org)

with a 6 channel Imager (figure 10.13). INSAT-3D Sounder channels are similar to those in GOES-12 Sounder and many of the spectral bands are similar to High resolution Infrared Radiation Sounder (HIRS) onboard NOAA-ATOVS. Observation in these Sounder channels can be used to retrieve profiles of temperature and moisture as well as total column estimates of ozone. Present algorithm for INSAT-3D Sounder is adapted from the operational HIRS and GOES algorithms developed by Cooperative Institute for Meteorological Satellite Studies (CIMSS), University of Wisconsin.

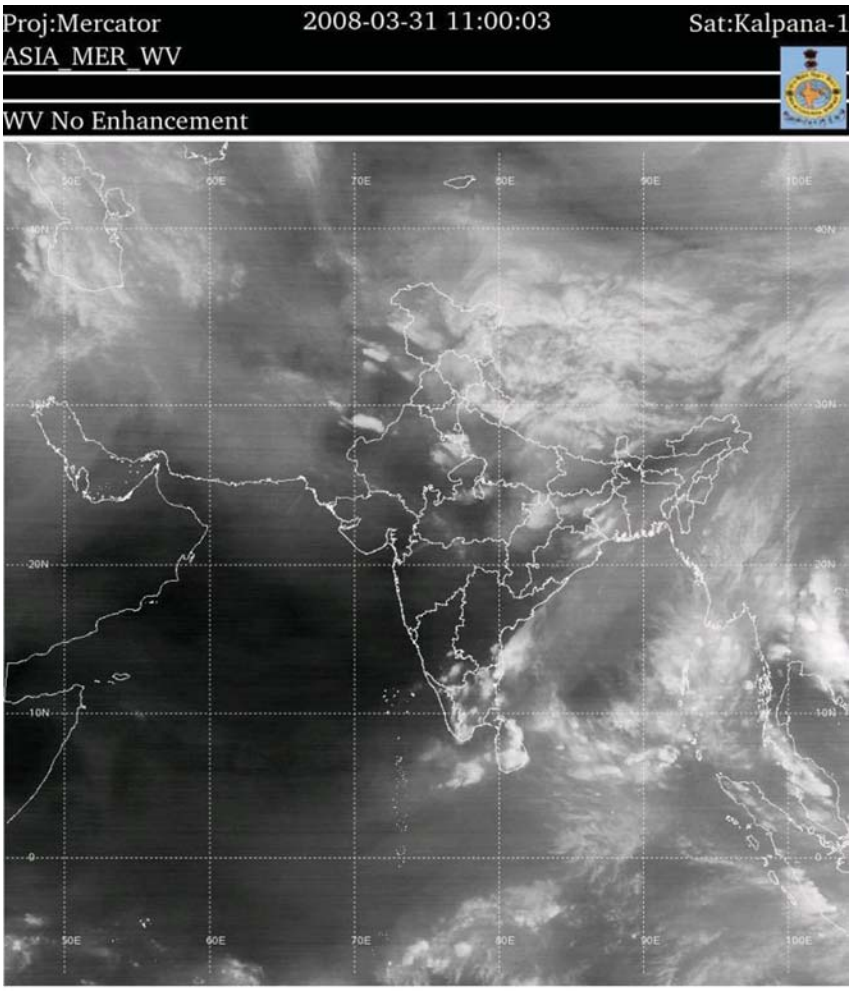

Figure 10.14: Water Vapour image from Kalpana-1 Satellite(source:www.imd.gov.in)

The use of geo-stationary water vapor imagery has allowed the determination of upper-level moisture content and determination of winds in cloud-free regions. The extraction of atmospheric motion vectors from satellite images (like IR & WV) has become most important component for operational numerical weather prediction (NWP). Satellite wind products are then assimilated in both regional and global-scale model and revealed its positive impacts on weather forecast (Kelly, 2004; Bedka and Mecikalski, 2005), especially over tropics. The availability of infrared window channel (10.5-12.5 µm) and water vapor channel (6.3 –7.1 µm) on-board KALPANA- VHRR, enabled us to derive cloud-tracked winds (900-100 hPa) and water vapor winds (500-100 hPa) from Indian geo-stationary satellites. The horizontal resolution of KALPANA- IR and WV channel is 8 Km (figure 10.14). Infrared images are used for detection and movement of clouds and for estimation of winds at different levels. The estimation of cloud motion vector (CMVs) wind is based on the assumption that clouds at different levels follow the atmospheric motion as rigid bodies. Three consecutive KALPANA-IR images at 30-minute interval are needed to determine the CMVs. The steps involved in these estimations are: i) Image Thresholding, ii) Feature Selection and Tracking, iii) Quality control and iv) Height assignment.

NASA's Mission to Planet Earth involves a variety of satellite and satellite sensors. Satellites presently in operation under this program are as follows:

Earth Radiation Budget Satellite (ERBS)

This satellite is primarily used for measuring visible radiation reflected by the earth and infrared energy emitted by the earth, including oceans, atmosphere and clouds. The principal experiments with ERBS include the Earth Radiation Budget Experiment (ERBE) and the Stratospheric Aerosol and Gas Experiment (SAGE).

Upper Atmosphere Research Satellite (UARS)

The UARS will carry out the first systematic, comprehensive study of the stratosphere and furnish important new data on the mesosphere and thermosphere. UARS chemistry and dynamics sensors will measure temperature, pressure, wind velocity, and concentrations of trace gas species in altitudes ranging from 15 to over 100 km. The UARS Data System Home Page gives an overview of the sensors, and more information can be obtained from

- The Halogen Occultation Experiment (HALOE)
- Microwave Limb Sounder (MLS)

- The Cryogenic Limb Array Etalon Spectrometer (CLAES)
- The Improved Stratospheric and Mesospheric Sounder (ISAMS)
- High Resolution Doppler Imager (HRDI)
- WINDII
- SOLSTICE
- The Solar Ultraviolet Spectral Irradiance Monitor (SUSIM)
- The Particle Environment Monitor (PEM)
- Active Cavity Radiometer Irradiance Monitor (ACRIM II)

TOPEX/Poseidon

Data from this satellite have been viewed in the unit on El Nino, since the TOPEX/Poseidon satellite is the key platform for ocean measurements such as ocean circulation (currents and tides), wave heights, and sea-surface height anomalies as well as atmospheric wind speed and water-vapor content over ocean areas.

The A-train satellite constellation (Figure 10.15), named after Aqua and Aura satellite has an orbit at an altitude of 705 km and inclination of ~98^{o}. Aqua leads the constellation with an equatorial crossing time of approximately 1:30 PM and data from these satellites provides a host of opportunity to understand aerosol cloud interactions.

10.5. MEGHA-TROPIQUES

Climate research on a global scale is a topic of worldwide interest and a necessity for general meteorological applications, weather prediction and ultimately useful in regional and global monitoring and protection of the earth's environment.

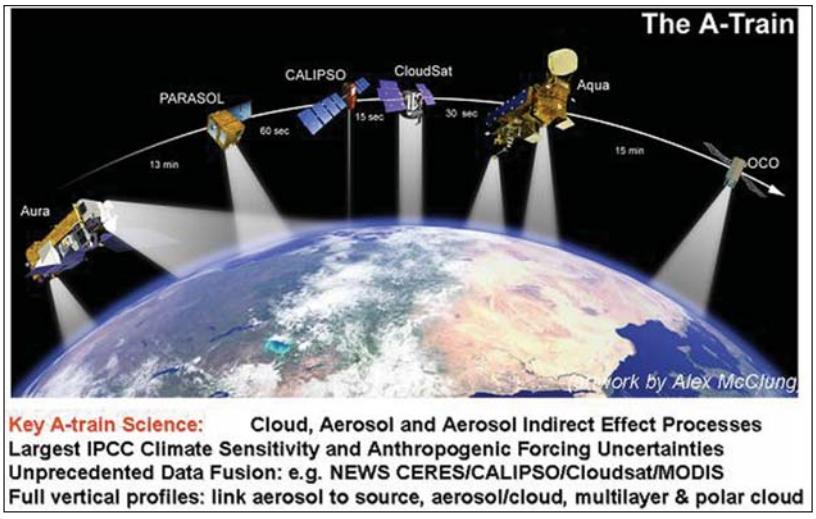

Figure 10.15: The EOS afternoon satellite constellation(source:http://www.gsfc.nasa.gov/gsfc/service/gallery/fact_sheets/earthsci)

Several satellite missions in the last three decades have demonstrated their potential utilization aspects in terms of instrument capabilities, accomplishment of science and application goals, and their merits for applying the data in weather forecasting and climate research. The currently operational space borne microwave imagers such as SSM/I, TMI (TRMM Microwave imager) and Oceansat-1 are a few examples of the keen interest and conviction on the capability, technology and performance of the passive microwave instruments for the atmospheric and oceanographic applications.

The Megha-Tropiques is a joint ISRO-CNES collaborative effort of developing and launching a small satellite and utilization of the data. This mission encompasses the development of three high technology payloads, viz. MADRAS (Microwave Analysis and detection of rain and atmospheric structure), SAPHIR (a 6-channel millimetrewave humidity sounder at 183.3GHz) and a scanner for radiation budget (ScaRaB). Prediction of the large scale variations in the tropical atmosphere is a very important aspect for climate research and meteorological applications. Particularly, measurements related to the Earth radiation budget, latent heat flux, water vapour, cloud liquid water and rainfall along with other parameters are of immense value for the climate models. High temporal frequency and large spatial coverage has been the emphasis in these applications.

The Megha-Tropiques mission is a joint ISRO-CNES programme for developing a small satellite carrying appropriate sensors for measuring the cloud and atmospheric parameters. Primarily, it carries three payloads: a microwave imager at 18, 23, 36, 89 and 157GHz, a millimetrewave sounder at 183.3GHz and a scanner for radiation budget measurements. The satellite is configured around the French Proteus bus and launched using the ISRO's PSLV launcher. The ISTRAC ground station at Bangalore is used for receiving and processing the science data.

Main objectives of the Megha-Tropiques mission:

The main objective of the Megha-Tropiques mission is to study the convective systems that influence the tropical weather and climate. The tropical region is the domain of monsoons, squall lines and tropical cyclones. It is also characterized by large intraseasonal, interseasonal and interannual variations, which may lead to catastrophic

events such as droughts and floods and change in energy and water budget of the Land-Ocean-Atmosphere system in the tropics has its influence on global climate.

The MEGHA- TROPIQUES mission aims to:

- provide simultaneous measurements of several elements of the atmospheric water cycle: water vapour, clouds, condensed water in clouds, precipitation and evaporation,
- Measure the corresponding radiative budget at the top of the atmosphere,
- Ensure high temporal sampling in order to characterize the life cycle of the convective systems and to obtain significant statistics

The main parameters to be measured by Megha-Tropiques are cloud cover, cloud top height, cloud albedo, cloud condensed water content, cloud ice content, rain rate, latent heat release, integrated water vapour content, profile of water vapour content, radiant fluxes at the top of the atmosphere, sea surface winds, sea surface temperature, sea surface evaporation fluxes, temperature profiles and 3D wind field.

The Megha-Tropiques satellite will be launched into an inclined orbit of 20 degrees and an altitude of 867 Km. The payloads are designed to provide large swahs with a high repetitively of three to six times a day depending on the latitudes. The frequency of observation is quite high in the inter-tropical zone between 10^0- 20^0 latitudes.

Mission Space Segment

The primary specifications of the satellite are highlighted below.

Spacecraft Bus	:	PROTEUS (French)
ORBIT	:	867 Km
Power available for payloads	:	~220 W
Onboard dat storage	:	2 GHz
Mission Life	:	3 Years (Design life: 5Years)
Inclination	:	20 deg
Launcher	:	PSLV (Dual satellite configuration)

The Megha-Tropiques mission envisages development of the three payloads, to measure the dynamic atmospheric variables which are

- A microwave imager: MADRAS (Microwave Analysis and Detection of Rain and Atmospheric Structure)
- A humidity sounder at 183.31GHz and
- ScaRaB (scanner for Radiation Budget:4 channels)

MADRAS

MADRAS is a five- frequency, 9-chanel mechanically scanning microwave imaging radiometric system. It has a mechanically scanning offset reflector, which scans the earth at a conical scan angle of ± 65 degrees resulting in

Table 10.3: Salient features of MADRAS

Frequencies	Polarization	Spatial Resolution	NE∆T(K) sensitivity at 300K	Absolute calibration	Inter Channel calibration (K)	Mission
18.7GHz	H+V	40±10%Km	0.7 K	±1 K	0.5 K	Rain Above Oceans
23.8GHz	V	40±10%Km	0.7 K	±1 K	0.5 K	Integrated water vapour
36.5GHz	H+V	40±10%Km	0.7 K	±1 K	0.5 K	Liquid water in clouds, rain above sea
89GHz	H+V	10±10%Km	1.1 K	±1 K	0.5 K	Convective rain areas over land and sea
157GHz (TBC)	H+V	6±10%Km	2K (TBC)	(TBC)	(TBC)	Ice at cloud tops

a ground swath of more then 1700 Km. The three low frequency channels at 18, 23 and 36 GHz have a coincident footprint of 40 Km. The 89 and 157 GHz have a resolution of 10 and 6 Km respectively.

The major specification of MADRAS are shown in table 10.3

SAPHIR

SAPHIR is mechanically scanning millimeter wave humidity sounder. It scans the earth in a nadir plane symmetrically with respect to the local vertical with a scan angle of $\pm 45^0$. The instrument has six channels in the water vapour line at 183 GHz with a footprint diameter of about 10 Km. The major specifications of SAPHIR are shown in table 10.4.

SCARAB

Table 10.4: Major specifications of SAPHIR

Central nominal frequencies (GHz)	Spatial Resolution	NEΔT(K) sensitivity requirement	NEΔT sensitivity goal	Polarisation
183.31±0.2	10 Km	2 K	1 K	V
183.31±1.1	10 Km	1.8 K	1 K	V
183.31±2.7	10 Km	1.8 K	1 K	V
183.31±4.2	10 Km	1.5 K	1 K	V
183.31±6.6	10 Km	1.5 K	1 K	V
183.31±11	10 Km	1.2 K	1 K	V

The SCARAB is a cross track scanning radiometer. This sensor has four channels operation in the 0.5 to 0.7μm, 0.2 to 4 μm, 0.2 to 200 μm and 10.5 to 12.5 μm spectral bands. SCARAB consists of two modules viz. the optical sensor module, which includes the scanner, and the calibration devices and the electronic module. Table 10.5 shows the specification of ScaRaB.

Table 10.5 : Major specifications of SCARAB

Channel	0.5 to 0.7 μm
SC1 - Visible	0.2 to 4 μm
SC2 -Solar	0.5 to 200 μm
SC3 -Total	0.5 to 0.7 μm
SC4 –IR Window	10.5 to 12.5 μm

Ground segment

The Megha-Tropiques spacecraft will be launched by PSLV in an 867 Km circular orbit having an inclination of 20^0. The spacecraft collects data from three major scientific payloads, namely MADRAS, ScaRaB and SAPHIR. The global scientific data from these payloads will be collected mainly from ISTRAC Bangalore.

The telemetry channel of the Proteus bus consists of a QPSK modulated single telemetry downlink having a bit rate of 727 kbps. The telemetry data consists of real time house keeping data of spacecraft and instrument health, stored house keeping and health data and the stored payload data.

References

Adler RF and Negri AJ, 1988, A satellite infrared technique to estimate tropical convective and stratiform rainfall, *Journal of Applied Meteorology*, **27**: 30-51.

Arkin PA, 1979, The relationship between fractional coverage of high cloud and rainfall accumulations during GATE over the B-scale array, *Monthly Weather Review*, **106**: 1153-1171.

Arkin PA and Xie P, 1994, The Global Precipitation Climatology Project: First algorithm intercomparison project, *Bulletin of American Meteorological Society,* **75**: 401–419.

Arkin PA and Meisner BN, 1987, The relationship between large-scale convective rainfall and cold cloud over the western hemisphere during 1982 - 1984, *Monthly Weather Review*, **115**: 51-74.

Ba MB and Gruber A, 2001, GOES Multispectral Rainfall Algorithm (GMSRA), *Journal of Applied Meteorology,* **40**:1500-1514.

Badarinath KVS, Kharol SK, Kaskaoutis DG, Sharma AR, Ramaswamy V and Kambezidis HD, 2010, Long-range transport of dust aerosols over the Arabian Sea and Indian region – a case study using satellite data and ground-based measurements, *Global and Planetary Change*, doi:10.1016/j.gloplacha.2010.02.003 (in Press).

Badarinath KVS, Kharol SK, Kaskaoutis DG and Kambezidis HD, 2007, Case study of a dust storm over Hyderabad area, India: Its impact on solar radiation using satellite data and ground measurements, *Science of the Total Environment*, **384**: 316-332.

Bedka KM and Mecikalski JR, 2005, Application of satellite-derived atmospheric motion vectors for estimating meso-scale flows, *Journal of Applied Meteorology*, **44**: 1761-1772.

Ferraro RR and Marks GF, 1995, The development of SSM/I rain-rate retrieval algorithms using ground-based radar measurements, *Journal of Atmospheric and Oceanic Technology,* **12**: 755–770.

Gairola RM and Krishnamurti TN, 1992, Rain rates based on OLR, SSM/I and rain gauge data sets, *Meteorology and Atmospheric Physics*, **50**: 165-174.

Gairola RM, Varma AK, Pokhrel S and Agarwal VK, 2004, Integrated satellite microwave and infrared measurements of precipitation during a Bay of Bengal cyclone, *Indian Journal of Radio & Space physics*, **33**: 115-124.

Kaplan LD, 1959, Inference of atmospheric structure from remote radiation measurements, *Journal of the Optical Society of America*, **49**: 1004.

Kelly G, 2004, Observing system experiments of all main data types in the ECMWF operational system, 3rd WMO Numerical Weather Prediction OSE Workshop, Alpbach, Austria, WMO, *Technical Report*, **1228**: 32-36.

King JIF, 1956, The radiative heat transfer of planet earth, *Scientific Use of Earth Satellites*, University of Michigan Press, Ann Arbor, Michigan, 133-136.

Kummerow C and Giglio, 1996, A simplified scheme for obtaining precipitation and vertical hydrometeor profiles from passive microwave sensors, *IEEE Transactions of Geosciences & Remote Sensing,* **34**: 1213-1232.

Liu G and Curry JA, 1992, Retrieval of precipitation from satellite microwave measurement using both emission and scattering, *Journal of Geophysical Research*, **97(9)**: 9959– 9974.

Menzel WP and Purdom JFW, 1994, Introducing GOES-I: The first of a new generation of geostationary operational environmental satellites, *Bulletin of American Meteorological Society,* **75**: 757-781.

Scofield RA and Kuligowski RJ, 2003, Status and outlook of operational satellite precipitation algorithms for extreme precipitation events, *Weather Forecasting*, **18**: 1037-1051.

Smith WL, Suomi VE, Menzel WP, Woolf HM, Sromovsky LA, Revercomb HE, Hayden CM, Erickson DN and Mosher FR, 1981, First sounding results from VAS-D, *Bulletin of American Meteorological Society,* **62**: 232-236.

Smith WL, Woolf HM, Hayden CM, Wark DQ and McMillin LM, 1979, The TIROS-N operational vertical sounder, *Bulletin on American Meteorological Society,* **60**: 1177-1187.

Torres O, Bhartia PK, Herman JR, Ahmad Z and Gleason J,1998, Derivation of aerosol properties from satellite measurements of backscattered ultraviolet radiation: Theoretical basis, *Journal of Geophysical Research*, **103** : 17099–17110

Vicente GA, Scofield RA and Menzel WP, 1998, The operational GOES infrared rainfall estimation technique, *Bulletin on American Meteorological Society*, **79**: 1883-1898.

Wark DQ, 1961, On indirect temperature soundings of the stratosphere from satellites, *Journal of Geophysical Research*, **66 (1)**: 77.

Wark DQ, Hilleary DT, Anderson SP and Fisher JC, 1970, Nimbus satellite infrared spectrometer experiments, *IEEE Transactions on Geosciences Electronics,* **8**: 264-270.

Wilheit T, Kummerow CD and Ferrao R, 2003, Rainfall algorithms for AMSR-E, *IEEE Transactions of Geosciences & Remote Sensing*, **41(2)**: 204-214.

http://www.gsfc.nasa.gov/gsfc/service/gallery/fact_sheets/earthsci/green.htm

http: //earthobservatory.nasa.gov/Features/Aerosols/

http://www.gsfc.nasa.gov/gsfc/service/gallery/fact_sheets/earthsci/green.htm

http://www.gsfc.nasa.gov/gsfc/service/gallery/fact_sheets/earthsci

http://www.esa.int

http://www.isro.org

http://www.imd.gov.in